

Fluorescence spectra of $\text{NH}_2 \tilde{X}^2B_1 \leftarrow \tilde{A}^2A_1 \Sigma$ bands: Experiment and theory

Carlo Petrongolo^{a)}

Dipartimento di Chimica, Universita' di Siena, Via A. Moro 2, I-53100 Siena, Italy

Haiyan Fan, Ionela Ionescu, David Kuffel, and Scott A. Reid

Department of Chemistry, Marquette University, Milwaukee, Wisconsin 53201-1881

(Received 21 February 2003; accepted 15 April 2003)

We report new calculations and measurements of fluorescence properties of the title system, which is important in astrochemical processes. Dispersed fluorescence spectra show extensive \tilde{X}^2B_1 vibrational progressions that depend on the initial \tilde{A}^2A_1 state. Observed and calculated $(0, \nu'_2, 0)\Sigma$ lifetimes are in good accord, save for $\nu'_2=4$ (bent molecule notation), and calculated $(1, \nu'_2 - 2, 0)\Sigma$ lifetimes are longer than the $(0, \nu'_2, 0)\Sigma$ ones. The calculated laser-induced fluorescence spectrum is compared with experimental absorption data and with previous calculations, finding that the present treatment underestimates the intensity of the $(0, 4, 0)\Sigma$ band. © 2003 American Institute of Physics. [DOI: 10.1063/1.1580112]

I. INTRODUCTION

Since the detailed analysis by Dressler and Ramsay,¹ the $\text{NH}_2 \tilde{X}^2B_1 \leftrightarrow \tilde{A}^2A_1$ electronic spectra have been extensively studied both experimentally² and theoretically.³ NH_2 is indeed a small molecule that allows detailed investigations, and is the best known example where Renner-Teller (RT) effects can be measured and calculated. Energy levels are known with great accuracy, but absorption and fluorescence intensities are much less well known, and depend critically on the initial state and its population. Experimentally, absorption intensities in the Ar matrix at 4.2 K,⁴ dispersed fluorescence (DF) spectra of the $\tilde{A}^2A_1(0, 4, 0)$ and $(0, 10, 0)\Pi$ bands (bent molecule notation),^{5,6} and radiative lifetimes⁷⁻⁹ τ up to $\sim 19000 \text{ cm}^{-1}$ have been measured. Theoretically, some transition dipole moments and lifetimes were calculated by Jungen *et al.*¹⁰ (JHM), Buenker *et al.*,¹¹ and Jensen *et al.*³ (JKB). The first two studies^{10,11} were limited to an effective one-dimension (1D) bending treatment, and while Ref. 3 is very recent, the published data allow one to obtain only a part of the absorption spectrum.

Using the bent molecule notation, this paper presents new theoretical and experimental studies concerning fluorescence properties of $\tilde{A}^2A_1(0, \nu'_2, 0)$ and $(1, \nu'_2 - 2, 0)\Sigma$ bands, which are quite important in astrochemical processes.¹² We calculated state-to-state fluorescence rates of DF spectra, radiative lifetimes, and laser-induced fluorescence (LIF) intensities, using a 3D vibrational method that neglects fully the molecular rotation but considers stretch-bend interactions. We compare the calculated τ with precise new measurements for Σ bands, reported here for the first time and encompassing levels up to $\nu'_2=12$ at $\sim 31000 \text{ cm}^{-1}$. RT effects are thus omitted in the theoretical study and are minimal for the observed values.

II. CALCULATIONS

Let $|i\rangle$ and $|f\rangle$ be the initial and final states of a fluorescence transition, $\hbar\omega_{fi}$ their energy difference, and $\boldsymbol{\mu}$ the electric dipole moment. Fluorescence rates γ_{fi} , lifetimes τ_i , and LIF intensities¹³ I_i^{LIF} are equal to

$$\gamma_{fi} = \frac{4|\psi_{fi}|^3}{3\hbar c^3} |\langle f|\boldsymbol{\mu}|i\rangle|^2, \quad \tau_i = 1 / \sum_f \gamma_{fi}, \quad (1)$$

$$I_i^{\text{LIF}} \propto \sigma_{i0}^{\text{ABS}} [1 - \exp(-t^{\text{acq}}/\tau_i)] \propto \omega_{i0} |\langle i|\boldsymbol{\mu}|0\rangle|^2 \times [1 - \exp(-t^{\text{acq}}/\tau_i)], \quad (2)$$

where σ_{i0}^{ABS} are absorption cross sections from the ground state $|0\rangle$ and t^{acq} is the acquisition time of the experiment.

Omitting the molecular rotation and using \tilde{X}^2B_1 and \tilde{A}^2A_1 multireference configuration-interaction potentials,¹⁴ Born-Oppenheimer Σ vibrational states and levels were calculated in primitive and optimized finite basis representations, as described in detail in Ref. 15. Levels up to $\sim 35000 \text{ cm}^{-1}$ above the ground one were converged within 0.1 cm^{-1} , employing 91 and 71 primitive functions for the stretching and bending modes, respectively, and 2556 and 1491 optimized functions for \tilde{X}^2B_1 and \tilde{A}^2A_1 , respectively. The active component of $\boldsymbol{\mu}$ is perpendicular to the NH_2 plane, and the electronic transition moment is approximated as¹⁰

$$\mu_{21} = \mu_0 \cos(\theta/2), \quad (3)$$

where 1 and 2 label \tilde{X}^2B_1 and \tilde{A}^2A_1 , respectively, μ_0 is a constant, and θ is the bending angle.

III. EXPERIMENTS

The apparatus consisted of a cubic, black-anodized aluminum vacuum chamber evacuated by a 6 in. water-baffled diffusion pump (Varian VHS-6) and equipped with a molecular beam source and laser induced fluorescence detection assembly. The NH_2 radicals were generated by a pulsed elec-

^{a)}Electronic mail: petrongolo@unisi.it

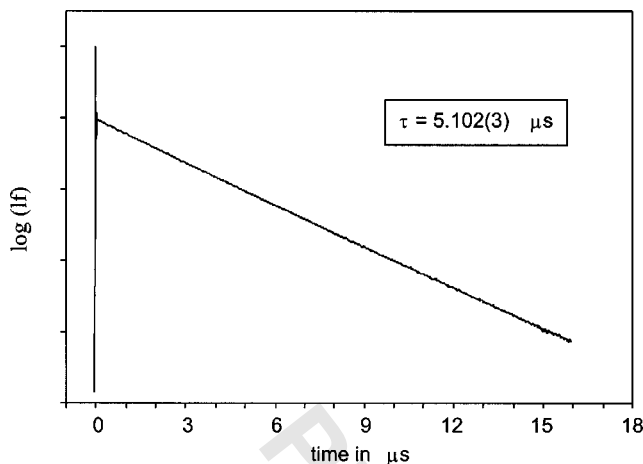


FIG. 1. Fluorescence decay observed following excitation of the F_1 component of the $2_{02} \leftarrow 1_{10}$ transition in the $\tilde{A}^2A_1(0,6,0)\Sigma$ band. The stated uncertainty represents one standard error.

trical discharge through a $\sim 1\%$ mixture of NH_3 in Ar that was premixed in a stainless steel cylinder. Details of the nozzle design were reported elsewhere.¹⁶ The typical backing pressure was ~ 1 bar, and discharge was initiated by an 800 V pulse of $\sim 15 \mu\text{s}$ duration that passed through a 10 k Ω ballast resistor. The timing of laser, nozzle, and discharge firing was controlled by a digital delay generator (Stanford Research Systems DG535), which generated the variable width gate pulse for the high voltage pulser (Directed Energy GRX-1.5K-E).

The laser system consisted of an etalon narrowed dye laser (Lambda-Physik Scanmate 2E) pumped by the second or third harmonic of an injection seeded Nd:YAG laser (Continuum Powerlite 7010). Wavelengths between ~ 320 and 375 nm were generated by doubling the dye laser output in a BBO crystal, while those between ~ 375 nm and 440 nm were generated by mixing the dye fundamental with the Nd:YAG fundamental in a second BBO crystal. Wavelengths between ~ 440 and 520 nm were generated via the use of appropriate dyes pumped with the Nd:YAG third harmonic. Typical pulse energies were ~ 200 – $300 \mu\text{J}$ in a ~ 3 mm diam beam. A quartz window was used to direct a portion of the dye laser fundamental into an Fe–Ne optogalvanic lamp for absolute wavelength calibration. The Nd:YAG laser frequency (9397.44 cm^{-1}) was determined by calibrating the sum frequency against lines of an Fe–Ar optogalvanic lamp.

The laser beam crossed the molecular beam at right angles at a distance of ~ 10 mm (~ 20 exit orifice diameters) downstream. Fluorescence was collected by a two-lens F/1.5 condenser assembly, and filtered via an appropriate long-pass cutoff filter (Corion) prior to striking a photomultiplier tube detector (Oriel) held at typically -600 V. The PMT signal was terminated into 50 Ω , and digitized at a typical sampling rate of 250 MHz. For lifetime measurements, the molecular beam was oriented at 180° to the detection assembly to minimize the effects of molecular fly-out from the detector field of view. This arrangement was found to give single exponential decays over several fluorescence lifetimes for all transitions probed, as illustrated in Fig. 1. The lifetime was deter-

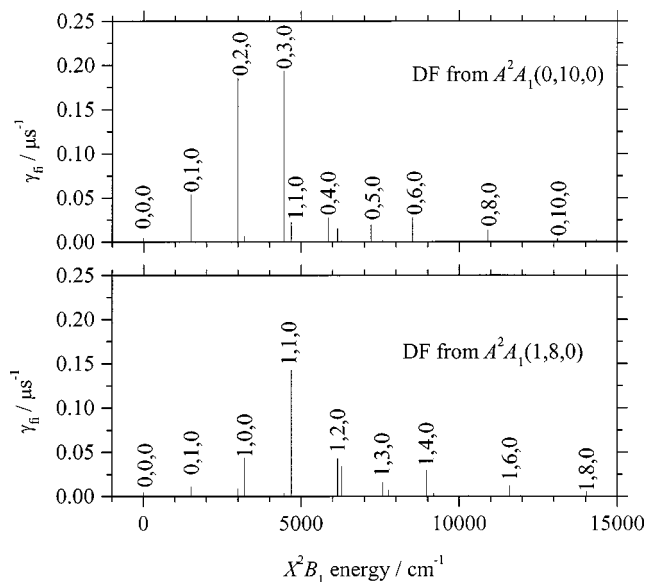


FIG. 2. Calculated DF spectra of the \tilde{A}^2A_1 bands $(0, 10, 0)\Sigma$ (upper panel) and $(1, 8, 0)\Sigma$ (lower panel), and \tilde{X}^2B_1 assignments.

mined via linear regression analysis over typically three or more fluorescence lifetimes. Waveforms were averaged over 2500 laser shots, with six waveforms typically collected for each transition.

IV. RESULTS AND DISCUSSION

Figure 2 reports the calculated state-to-state fluorescence rates γ_{fi} (DF spectra) of the high lying $\tilde{A}^2A_1 \Sigma$ bands $(0,10,0)$ and $(1,8,0)$. Because both initial \tilde{A}^2A_1 states are quite excited, their DF spectra show long and inverted progressions of the final \tilde{X}^2B_1 vibrational species. The first spectrum is dominated by the $\tilde{X}^2B_1(0, \nu_2'')$ bending progression, which peaks at $\nu_2''=2$ and 3, and extends up to $\nu_2''=10$. It also shows some weaker $\tilde{X}^2B_1(1, \nu_2'')$ bands for $\nu_2'' \leq 2$, and is in good agreement with the experimental DF spectrum of $\tilde{A}^2A_1(0,10,0)\Pi$.⁶ On the contrary, the \tilde{A}^2A_1 state with $\nu_1'=1$ decays mostly towards $\tilde{X}^2B_1(1, \nu_2'')$ stretch–bend bands, populating preferentially the $(1,1,0)$ level owing to the common symmetric-stretch excitation. These different product distributions thus allow a clear observation of two \tilde{X}^2B_1 vibrational progressions. The rates γ_{fi} depend more on the transition moments μ_{fi} than on the frequencies $|\omega_{fi}|$ and are larger for $\nu_1'=0$ than for $\nu_1'=1$, because the pure bending \tilde{A}^2A_1 species has larger μ_{fi}^2 with \tilde{X}^2B_1 states and emits preferentially higher-frequency photons. This behavior is general for $\tilde{A}^2A_1(0, \nu_2')$ and $(1, \nu_2', -2, 0)$ bands, is preferred at low ν_2' where the vibrational mixing is small, and is the origin of the smaller lifetimes of the $(0, \nu_2', 0)$ progression with respect to the $(1, \nu_2', -2, 0)$ one, as we shall see below.

Table I provides a summary of the measured lifetimes τ_i for Σ bands, which decrease from $\sim 8 \mu\text{s}$ for $(0,4,0)$ to $\sim 1.6 \mu\text{s}$ for $(0,12,0)$, reflecting the cubic energy dependence of the spontaneous emission rate. Little variation with rotational or

TABLE I. Measured fluorescence lifetimes for $\tilde{A}^2A_1 \Sigma$ bands.

Band	Transition	$\tau/\mu\text{s}$
(0,4,0)	$2_{02} \leftarrow 1_{10}(F_1)$	7.804(8) ^a
	$1_{01} \leftarrow 1_{11}(F_1)$	7.920(10)
	$0_{00} \leftarrow 1_{10}$	7.523(12)
(0,6,0)	$2_{02} \leftarrow 1_{10}(F_2)$	5.188(20)
	$1_{01} \leftarrow 1_{11}(F_1)$	5.272(19)
	$0_{00} \leftarrow 1_{10}$	5.091(20)
(0,7,0)	$3_{03} \leftarrow 2_{11}(F_1)$	2.775(13)
	$2_{02} \leftarrow 1_{10}(F_2)$	3.232(13)
	$1_{01} \leftarrow 1_{11}(F_2)$	3.489(18)
	$0_{00} \leftarrow 1_{10}$	3.427(14)
(0,8,0)	$3_{03} \leftarrow 2_{11}(F_1)$	3.245(13)
	$2_{02} \leftarrow 1_{10}(F_2)$	3.319(6)
	$1_{01} \leftarrow 1_{11}(F_1)$	3.297(8)
	$0_{00} \leftarrow 1_{10}$	3.312(17)
(0,9,0)	$2_{02} \leftarrow 1_{10}(F_1/F_2)$	2.935(14)
	$1_{01} \leftarrow 1_{11}(F_1)$	2.630(4)
	$0_{00} \leftarrow 1_{10}$	2.920(30)
(0,10,0)	$2_{02} \leftarrow 1_{10}(F_1)$	2.522(24)
	$1_{01} \leftarrow 1_{11}(F_1/F_2)$	2.444(10)
	$0_{00} \leftarrow 1_{10}$	2.158(25)
(0,11,0)	$1_{01} \leftarrow 1_{11}(F_1/F_2)$	1.880(5)
	$0_{00} \leftarrow 1_{10}$	1.847(4)
(0,12,0)	$0_{00} \leftarrow 1_{10}$	1.605(8)

^aOne standard error in parentheses.

spin-rotational state is observed, as we avoided including lifetimes for any rovibronic levels that could be identified as perturbed from our fluorescence excitation measurements.¹⁶ Despite the fact that the molecule is undergoing large-amplitude bending motion, such perturbations are relatively sparse for the low rotational levels ($N \leq 3$) accessed in our experiment. For the $\tilde{A}^2A_1(0,4,0)\Sigma$ band, we measure an average $\tau = 7.749(18) \mu\text{s}$, 2.3 μs lower, but considerably more precise than the $10.0 \pm 1.7 \mu\text{s}$ of Ref. 7.

We compare in Fig. 3 experimental (averaged values of Table I, full line) and calculated (dotted line) lifetimes of

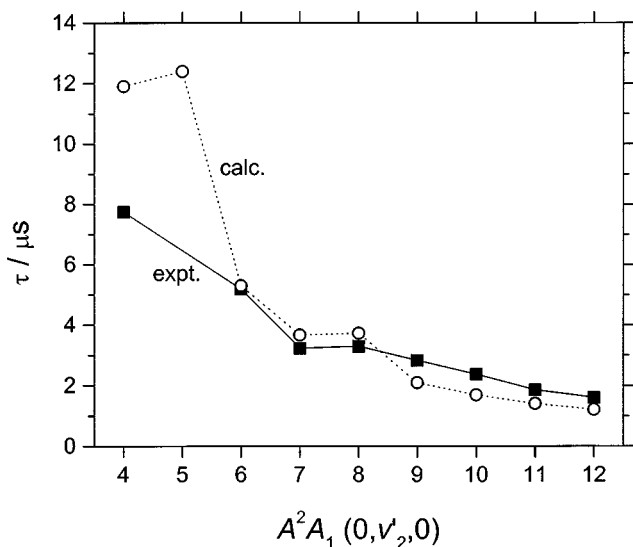


FIG. 3. Measured (averaged values of Table I, full line) and calculated (dotted line) lifetimes of $\tilde{A}^2A_1(0, \nu'_2, 0)\Sigma$ bands. Note that the $\nu'_2=5$ level is actually a (0,5,0)–(1,3,0) Fermi resonance.

TABLE II. Calculated fluorescence lifetimes (μs) for $\tilde{A}^2A_1(0, \nu'_2, 0)$ and $(1, \nu'_2-2, 0)\Sigma$ bands.

ν'_2 (bent notation)	(0, $\nu'_2, 0$)		(1, $\nu'_2-2, 0$)
	This work	Ref. 10 ($\mu_0=0.2855$ a.u.)	This work
0	219.9	204.3	
1	97.8	67.3	
2	40.5	30.8	113.7
3	22.0	17.1	88.2
4	11.9	10.7	35.0
5	12.4	7.2	12.8
6	5.3	5.2	9.9
7	3.7	3.9	12.9
8	3.7	3.0	5.2
9	2.1	2.4	3.6
10	1.7		2.7
11	1.4		2.1
12	1.2		1.7

$\tilde{A}^2A_1(0, \nu'_2, 0)\Sigma$ bands, plotting also the calculated τ ($\nu'_2=5$) that was not measured here. The calculated τ were fitted to those observed, finding $\mu_0=0.3035$ a.u. in Eq. (3). This value gives a transition moment $\mu_{21}=0.19$ a.u. at the ground state equilibrium angle of 102.4° , smaller than the recent JKB (Ref. 3) *ab initio* value of 0.29 a.u., but in agreement with 0.18 and ~ 0.20 a.u. of Refs. 10 and 11. Figure 3 shows that the calculated lifetime at $\nu'_2=4$ is overestimated with respect to the observed one, owing to a too small transition moment with the $\tilde{X}^2B_1(0,0,0)$ state. The agreement between calculated and observed τ is better at $\nu'_2=6, 7$, and 8, and then decreases slightly at higher bending quanta, where the calculated lifetimes are systematically smaller by $\sim 26\%$. This last finding suggests that some weak interactions may be present in the high-energy spectrum, possibly of rovibronic or Fermi-resonance type, which the calculations underestimate. Overall, the calculated lifetimes have an average error of $\sim 23\%$, which is certainly acceptable given the approximations of the theoretical treatment and the large errors that calculated τ can have.¹³

Table II reports \tilde{A}^2A_1 lifetimes of the $(0, \nu'_2, 0)\Sigma$ and $(1, \nu'_2, -2, 0)\Sigma$ progressions, calculated both in the present work and in JHM (Ref. 10) with a 1D bending model. We use $\mu_0=0.2855$ a.u. for the JHM data, according to their Eqs. (15) and (18). The present τ values of the $(1, \nu'_2, 0)\Sigma$ bands have been obtained for the first time. Our calculated τ for $\nu'_2=2$ and 3 are in good agreement with the experimental values of 45.6 ± 5.7 and $23 \pm 9^{41} \mu\text{s}$, respectively,^{7,8} and our calculated lifetimes of $\nu'_2=5$ and 8 are larger than those of $\nu'_2=4$ and 7, respectively, contrary to the inverse cubic energy dependence of τ . The bands with $\nu'_2=5$ and 8 have indeed a mixed bending-symmetric stretch character, owing to (0,5,0)–(1,3,0) and (0,8,0)–(1,6,0) Fermi resonances that increase their lifetimes. This finding explains why the average observed lifetime of $\nu'_2=8$ is slightly longer than that of $\nu'_2=7$ (Table I). Our calculated τ ($\nu'_2=5$) is larger than that measured in another work ($8.1 \pm 2 \mu\text{s}$),⁷ probably because the present calculations overestimate the strength of the (0,5,0)–(1,3,0) Fermi resonance.

As expected, the JHM (Ref. 10) lifetimes are smaller

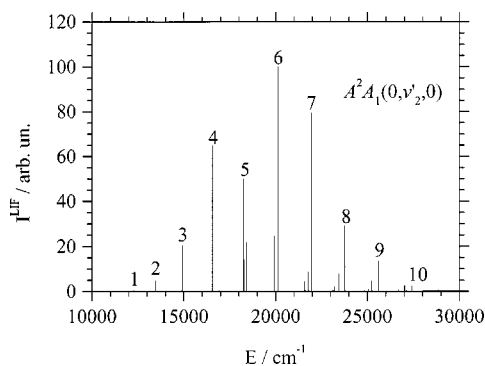


FIG. 4. Calculated LIF spectrum of $\tilde{A}^2A_1\Sigma$ bands and ν'_2 quanta of the $(0, \nu'_2, 0)$ bands. The intensity of the strongest band $(0, 6, 0)$ is equal to 100 arbitrary units.

than ours (save for $\nu'_2=9$), because that previous work neglects bend–stretch interactions that increase τ .

For $2\nu'_1 + \nu'_2 \leq 8$, $\tau(\nu'_1=1)$ are up to four times larger than those of the pure bending bands, except for the Fermi resonances $(0, 5, 0) - (1, 3, 0)$ and $(0, 8, 0) - (1, 6, 0)$. As shown above, this result is due to $(0, \nu'_2, 0)$ preferred Franck–Condon access to lower \tilde{X}^2B_1 vibrational states. For $2\nu'_1 + \nu'_2 \geq 9$, this trend is somewhat reduced, owing to the mixings of the vibrational modes and the general lowering of τ at high energies. We also remark that there is a striking similarity between the calculated lifetimes of $(0, \nu'_2, 0)$ and $(1, \nu'_2, 0)$, which suggests that τ is strongly governed by the ν'_2 bending quantum number, except for $(1, 3, 0)$ in Fermi-resonance with $(0, 5, 0)$.

Figure 4 shows the $\tilde{X}^2B_1 \leftarrow \tilde{A}^2A_1$ calculated LIF spectrum of Σ bands, obtained with an acquisition time $t^{\text{acq}} = 16 \mu\text{s}$ according to Fig. 1. As in the gas-phase absorption spectrum,⁴ the LIF intensity is dominated by a long and regular $\tilde{A}^2A_1(0, \nu'_2, 0)$ bending progression, owing to very different equilibrium θ values of the electronic states. The intensity dip at $\nu'_2=5$ is due to the $(0, 5, 0) - (1, 3, 0)$ Fermi resonance, and the strongest LIF intensity at $\nu'_2=6$ is consistent with the largest calculated absorption intensity for this state. Satellite lines of each $\tilde{A}^2A_1(2\nu'_1 + \nu'_2)$ polyad correspond to symmetric stretch–bending combination bands $(1, \nu'_2, -2, 0)$, and the polyads are well separated in energy up to $\sim 27\,000 \text{ cm}^{-1}$, i.e., the vibrational spectrum does not show significant perturbations save that at $\nu'_2=5$.

The calculated LIF and absorption intensities are maximal at $\nu'_2=6$, whereas the strongest feature observed in gas-phase absorption corresponds to $(0, 4, 0) \Sigma$ bands.¹ This difference is mainly due our potentials that were calculated for describing the $\text{N} + \text{H}_2$ collision,¹⁴ and thus behave correctly in the full configurational space but are not optimized for spectroscopic purposes. Molecular rotation, and therefore selection rules $J=0 \leftarrow | \rightarrow J=0$ and $\Delta K = \pm 1$ and RT effects,

should be also important, because NH_2 absorption^{1,4} and fluorescence¹⁷ intensities depend strongly on the initial $|i\rangle$ and final $|f\rangle$ rotational states, on the population of $|i\rangle$, and on whether NH_2 is in thermal equilibrium or not.

Optimizing the potentials with respect to the observed bands and taking into account the RT coupling, JHM (Ref. 10) and JKB (Ref. 3) correctly found that the maximum absorption intensity is due to the Σ band with $\nu'_2=4$. Using Eq. (2) and the JHM lifetimes of Table II, the maximum LIF intensity calculated in Ref. 10 is for the $(0, 5, 0)\Sigma$ band.

Equation (3) of the electronic transition moment is another, minor source of calculation error, because $\cos(\theta/2)$ overweighs bent geometries, whereas the \tilde{A}^2A_1 vibrational states are maximal at linearity. Assuming a constant μ_{21} , in agreement with the Condon approximation but in contrast to the selection rule that imposes a zero moment at linearity, the $\tilde{A}^2A_1(0, 4, 0)$ band is preferred in absorption.

Calculations of fluorescence spectra using the JKB (Ref. 3) vibronic transition moments, which take into account the molecular rotation and the RT coupling, and comparisons with lifetime measurements for $K \geq 0$ are currently in progress.

ACKNOWLEDGMENTS

We thank P. Defazio for the assignment of the bands and J. Xin for useful discussions. This work has been supported by MIUR, University of Siena, IPCF-CNR of Pisa, and by the National Science Foundation under Grant No. CHE-9702803.

- ¹K. Dressler and D. A. Ramsay, *Philos. Trans. R. Soc. London, Ser. A* **251**, 553 (1959).
- ²I. Hadj Bachir, T. R. Huet, J.-L. Destombes, and M. Vervloet, *J. Mol. Spectrosc.* **193**, 326 (1999), and references therein.
- ³P. Jensen, W. P. Kraemer, and P. R. Bunker, *Mol. Phys.* **101**, 613 (2003), and references therein.
- ⁴G. W. Robinson and M. McCarty, *J. Chem. Phys.* **30**, 999 (1959).
- ⁵M. Kroll, *J. Chem. Phys.* **63**, 319 (1975).
- ⁶J. Schleipen, J. J. Ter Meulen, and M. Vervloet, *Chem. Phys. Lett.* **197**, 165 (1992).
- ⁷J. B. Halpern, G. Hancock, M. Lenzi, and K. H. Welge, *J. Chem. Phys.* **63**, 4808 (1975).
- ⁸V. M. Donnelly, A. P. Baronavski, and J. R. McDonald, *Chem. Phys.* **43**, 283 (1979).
- ⁹S. Mayama, S. Hiraoka, and K. Obi, *J. Chem. Phys.* **80**, 7 (1984).
- ¹⁰C. Jungen, K.-E. J. Hallin, and A. J. Merer, *Mol. Phys.* **40**, 25 (1980).
- ¹¹R. J. Buenker, M. Peric, S. D. Peyerimhoff, and R. Marian, *Mol. Phys.* **43**, 987 (1981).
- ¹²H. Kawakita, K. Ayani, and T. Kawabata, *Publ. Astron. Soc. Jpn.* **52**, 925 (2000).
- ¹³F. Santoro and C. Petrongolo, *J. Chem. Phys.* **111**, 9651 (1999).
- ¹⁴F. Santoro, C. Petrongolo, and G. C. Schatz, *J. Phys. Chem. A* **106**, 8276 (2002).
- ¹⁵E. Leonardi, C. Petrongolo, G. Hirsch, and R. J. Buenker, *J. Chem. Phys.* **105**, 9051 (1996).
- ¹⁶J. Xin, H. Fan, I. Ionescu, C. Annesley, and S. A. Reid, *J. Mol. Spectrosc.* (in press).
- ¹⁷V. M. Donnelly, A. P. Baronavski, and J. R. McDonald, *Chem. Phys.* **43**, 271 (1979).